

*Chapter 5***DYE MOLECULES IN ZEOLITE L NANO CRYSTALS
FOR EFFICIENT LIGHT HARVESTING***Gion Calzaferri*

*Department of Chemistry and Biochemistry, University of Bern,
Freiestrasse 3,
CH-3000 Bern 9, Switzerland*

SUMMARY

Zeolite nano crystals can act as hosts for supramolecular organization of molecules, complexes and clusters, thus encouraging the design of precise functionalities. The main role of the zeolite framework is to provide the desired geometry for arranging and stabilizing the incorporated species. Focusing on supramolecularly organized dye molecules in the channels of hexagonal zeolite L crystals we have shown that they provide fascinating possibilities for building an artificial *antenna device* which consists of highly concentrated monomeric dye molecules in a specific geometrical arrangement. Organic dyes have the tendency to form aggregates already at low concentration. Such aggregates are known to cause fast thermal relaxation of electronic excitation energy. The role of the zeolite is to prevent this aggregation and to superimpose a specific organization. Provided an appropriate dimension of dye molecules, they are oriented with respect to the channels of the zeolite and they cannot glide past each other because the linear channels are too narrow. This allows the filling of specific parts of the nano crystals with a desired type of dye. In such an antenna, light is absorbed by one of the strongly luminescent chromophores. Due to short intermolecular distances and the orientation of the electronic transition dipole moments with respect to the channels, the excitation energy is transported by Förster type energy migration preferentially along the axis of the cylindrical antenna to a specific trap. One can observe the alignment of the dyes in the channels by means of a polarizer. The fascination properties of the systems discussed in this article give rise to many speculations on potential applications. They can perhaps be used for realizing a new type of photovoltaic device in which the absorption of light and the creation of an electron-hole pair are spatially separated. Contributions to new imaging techniques, data storage, specific biological and medical applications can be imagined. The antenna nano crystals can also be regarded as candidates for realizing a new type of electronic screen with high spatial resolution. The extremely fast energy migration, the pronounced anisotropy, the geometrical constraints and the high concentration of monomers which can be realized have much potential in leading to new photo physical phenomena.

1. INTRODUCTION

Plants are masters in the direct transformation of sunlight into energy. In the ingenious antenna system of the leaf, sunlight is transported by chlorophyll molecules for the purpose of energy transformation. We have now succeeded in reproducing a similar light transport in an artificial system on a nano scale. In this artificial system, zeolite cylinders adopt the antenna function. The light transport is made possible by specifically organized dye molecules which mimic the natural function of chlorophyll. Zeolites, some of which occur in nature as a component of the soil, are materials with different cavity structures.¹⁻³ We are using miniature zeolite L crystals of cylindrical morphology which show a continuous tube system and we have succeeded in filling each individual tube with a chain of joined dye molecules. Light shining on the cylinder is first absorbed and then transported by the dye molecules inside the tubes to the cylinder end. Tests have shown that this radiationless transport takes place much faster than has been known for green plants so far,^{4,5} for which, however, other ultra fast processes have been reported.⁶ Attempts are being made to use the efficient zeolite-based light harvesting system for the development of a new type of thin layer solar cell in which the absorption of light and the creation of an electron-hole pair are spatially separated as in the natural antenna system of green plants.⁷ We expect that our system can also contribute to a better understanding of the important light harvesting process which plants use for the photochemical transformation and storage of solar energy.

We have synthesized nanocrystalline zeolite L cylinders ranging in length from 30 nm to about 3000 nm.⁸ A cylinder of 600 nm diameter e.g. consists of about 100'000 parallel arranged tubes.⁹⁻¹¹ Single red emitting dye molecules (oxonine) were put at each end of the tubes filled with green emitting dye (pyronine). This form of arrangement made an experimental proof of efficient light transport possible. Light of appropriate wavelength shining on the cylinder is only absorbed by the pyronine and moves along these molecules until it reaches the oxonine. The oxonine absorbs the energy by a radiationless energy transfer process, but it is not able to send it back to the pyronine. Instead it emits the energy in the form of red light, visible to the naked eye.^{9,10,12} The artificial light harvesting system makes it possible to realize a device in which the dye molecules inside the tubes are arranged in such a way that the whole light spectrum can be used by conducting light from blue to green to red without significant loss as illustrated in Scheme 1. Such a material could conceivably be used in a dye laser of extremely small size.^{7,13} The light harvesting nano crystals are also investigated as probes in near field microscopy and as luminescent probes in biological systems.



Scheme 1: Representation of a bi-directional antenna; $\lambda_1 < \lambda_2 < \lambda_3$. A cylindrical zeolite L nanocrystal containing in the middle part blue emitting dye molecules followed on both sides by green and then by red emitting ones. All dyes are present as monomers and the spectral overlap between the absorption and the emission spectra are large.

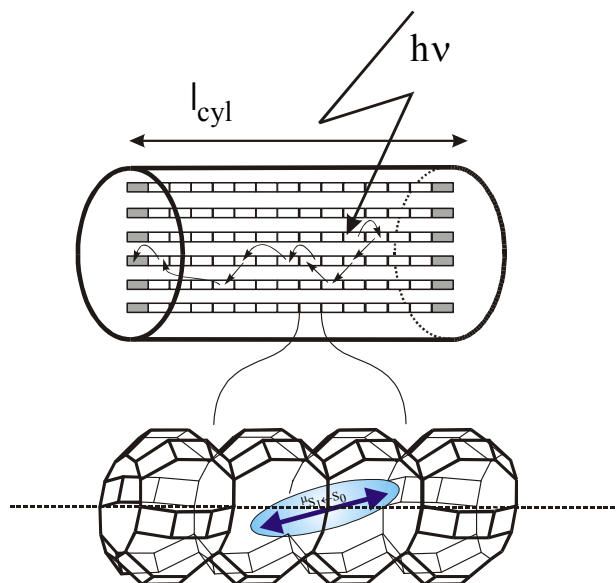
Synthesis, characterization, and applications of an artificial antenna for light harvesting within a certain volume and transport of the electronic excitation energy to a specific place of molecular dimension has been the target of research of many laboratories in which different

approaches have been followed.^{14,15} However, to our knowledge the system reported in ref 10 is the first artificial antenna which works well enough to deserve this name. Many other highly organized dye-zeolite materials of this type can be prepared by similar methods and are expected to show a wide variety of remarkable properties. The largely improved chemical and photochemical stability of dye molecules intercalated in an appropriate zeolite framework allows us to work with dyes which otherwise would be considered uninteresting because of lack of stability. We have developed two methods for preparing well defined dye-zeolite materials, one of them working at the solid/liquid and the other at the solid/gas interface.⁷ Different approaches for preparing similar materials are e.g. in situ synthesis¹⁶ or different types of crystallization inclusion synthesis.¹⁷

2. Basic Principles

Zeolite nano crystals can act as hosts for supramolecular organization of molecules, complexes, and clusters, thus encouraging the design of precise functionalities. The main role of the zeolite framework is to provide the desired geometry for arranging and stabilizing the incorporated species.^{7,18-20} Focusing on supramolecularly organized dye molecules in the channels of hexagonal zeolite L crystals we have shown that they provide fascinating possibilities for building an artificial *antenna device* which consists of highly concentrated monomeric dye molecules in a specific geometrical arrangement.²¹ Organic dyes have the tendency to form aggregates already at low concentration. Such aggregates are known to cause fast thermal relaxation of electronic excitation energy. The role of the zeolite is to prevent this aggregation and to superimpose a specific organization. Dye molecules of appropriate size are arranged with their long molecular axis along the linear channels and they cannot glide past each other because the linear channels are too narrow. This allows the filling of specific parts of the nano crystals with a desired type of dye. In such an antenna, light is absorbed by one of the strongly luminescent chromophores. Due to short distances and the ordering of the electronic transition dipole moments of the dyes with respect to the channels, the excitation energy is transported by Förster type energy migration preferentially along the axis of the cylindrical antenna to a specific trap. Classical aspects of energy transfer in molecular systems were described by H. Kuhn.²² We have recently demonstrated that the insertion of pyronine and oxonine molecules into the linear channels of zeolite L can be visualized with the help of a fluorescence microscope.⁹ One can observe the optical anisotropy of the material easily by means of a polarizer.

Theoretical considerations of energy migration as a series of Förster energy transfer steps have shown that in material of this kind energy migration rate constants of up to 30 steps/ps or even more can be expected.¹² The principle of the system investigated is illustrated in Scheme 2, where the empty bars represent donor molecules, e.g. pyronine, located in the channels of zeolite L and the dashed bars are acceptor molecules, e.g. oxonine, which act as luminescent traps at both ends of the cylinder. We define the occupation probability p as the ratio between the number of sites occupied by a dye and the total number of sites available. Hence, p adopts values between 0 for an unloaded zeolite and 1 for a zeolite loaded to its maximum. A nanocrystal of 600 nm length and a diameter of 800 nm gives rise to about 170'000 parallel-lying channels, each of which bears a maximum of 400 sites for molecules of the size of oxonine and pyronine.



SCHEME 2: Representation of a cylindrical nanocrystal consisting of organized dye molecules acting as donors (empty rectangles), and a trap at the front and the back of each channel, indicated by the shaded rectangles. The enlargement shows a detail of the zeolite L channel with a dye molecule and its electronic transition moment, the orientation of which depends on the type of molecules used (size and shape).

In the experiments reported in ref 10, light is absorbed by a pyronine molecule located somewhere in one of the channels. The excitation energy then migrates along the axis of the nanocrystal, as indicated by the arrows in Scheme 2, and is eventually trapped by an oxonine located at the front or at the back of the cylinder. The electronically excited oxonine then emits the excitation energy with a quantum yield of approximately one. This process which we call frontback trapping has been investigated theoretically for energy migration occurring by Förster energy transfer. We found that a total front trapping efficiency of up 99.8 % can be obtained for nano crystals of 50 nm length, if all sites are occupied by a pyronine chromophore.¹² The experiments reported in ref 10 are based on the fact that pyronine loaded zeolite L nanocrystals, modified with one oxonine molecule at the front and at the back of each channel on average as illustrated in Scheme 2 can be prepared and that it is possible to synthesize zeolite L nano crystal-cylinders of different average length with narrow size distribution.

For some applications it is desirable or even necessary to arrange the nano crystals as monolayers on a substrate such as a semiconductor, a conducting glass or a metal. This is explained in Figure 1 where as an example a potential new type of a dye-sensitized solar cell is illustrated. In such a device all incoming light is absorbed within the volume of the nano crystals of less than 1 μm length containing appropriate dye molecules for light harvesting. The excitation energy is then transported via very fast energy migration to the contact surface with the semiconductor, where, by efficient (radiationless) energy transfer from an excited dye to the semiconductor, it creates an electron hole pair in the semiconductor. This means that the absorption of light and the creation of an electron-hole pair are spatially separated similar as in the natural antenna system of green plants. The semiconductor could for instance consist of a very thin Si layer which by itself would be much too thin to absorb a

significant amount of light. The electron hole pair can then be separated as in an ordinary Si based solar cell. This results in a very thin solar cell of only a few μm thickness; see ref 7. We have shown that monocrystal-layers, of the type needed for realizing such a device, can be formed with zeolite A²³ and I am confident that the same will be possible with zeolite L and other zeolite nano crystals bearing the appropriate morphology, see e.g. Figure 1 in ref 11. For such a device monodirectional antenna nano crystals are needed, while in plastic solar cells and devices based on nano or microporous materials, the bi-directional antenna as illustrated in Scheme 1 can be used.

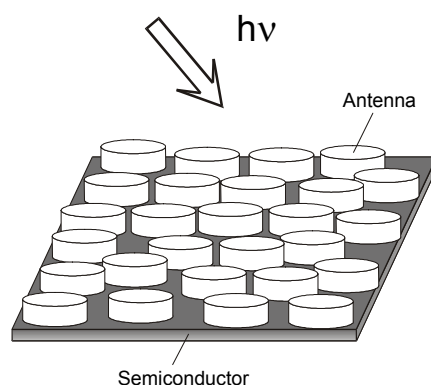


Figure 1. Speculation on a new type of dye-sensitized solar cell. The cylinders represent dye-loaded zeolite L nano crystals of about 600 nm length.

3. AN ELEGANT EXPERIMENT FOR VISUAL PROOF OF ENERGY TRANSFER

A simple experiment for the visual proof of the energy transfer between dyes in zeolite L is based on the observation that pyronine and oxonine dyes are incorporated from an aqueous solution with about equal rates. It is therefore possible to realize the situation illustrated in Figure 3 in which the donors are pyronine and the acceptors oxonine molecules. The mean distance between donors D and acceptors A can easily be varied by varying the occupation probability. To carry out the experiment we have two possibilities: The first is to work with a constant total amount of oxonine and pyronine and to vary the amount of zeolite L. The second is to work with a constant amount of zeolite L but to vary the amount of oxonine and pyronine. Both lead to dye loaded zeolite L nano crystals with varying occupation probability and therefore varying donor to acceptor distances. In aqueous dispersions the first type of experiments give nicer results for visual demonstration while the second possibility is more satisfactory for quantitative investigations because light scattering is constant for each sample. We now consider the visual demonstration. The five suspensions illustrated in Figure 2 have been prepared by starting with aqueous solutions containing exactly the same amount oxonine and pyronine (10^{-6} M). To 2.5 mL of these solutions a decreasing amount of zeolite L (average length of the nano crystals 300 nm) was added: **1**, 10 mg; **2**, 4 mg; **3**, 2 mg; **4**, 1 mg; **5**, 0.5 mg. Under these conditions incorporation of the dyes is quantitative when boiling the samples under reflux for 2 h.⁹ The concentration of each dye inside of the nano crystals

was **1**, 5×10^{-4} M; **2**, 1.25×10^{-3} M; **3**, 2.5×10^{-3} M; **4**, 5×10^{-3} M; **5**, 1.0×10^{-2} M. A rough estimate of the mean donor to acceptor distance R_{DA} can be obtained by assuming isotropic conditions:

$$R_{DA} = \left[\frac{3}{4\pi} \frac{1}{c_A N_A} \right]^{1/3} \quad (1)$$

N_A is the Avogadro number and c_A is the concentration of the oxonine in the zeolite nanocrystal. From this we obtain the following mean donor-acceptor distances: **1**, 93 Å; **2**, 68 Å; **3**, 54 Å; **4**, 43 Å; **5**, 34 Å. A more sophisticated theoretical treatment, which takes the anisotropy of the material into account can be found in ref. 12. The Förster radius for pyronine to oxonine energy transfer in a medium of refractive index of 1.4 is about 70 Å, based on the pyronine-oxonin spectral overlap which is $1.5 \times 10^{-13} \text{ cm}^3 \text{ M}^{-1}$.

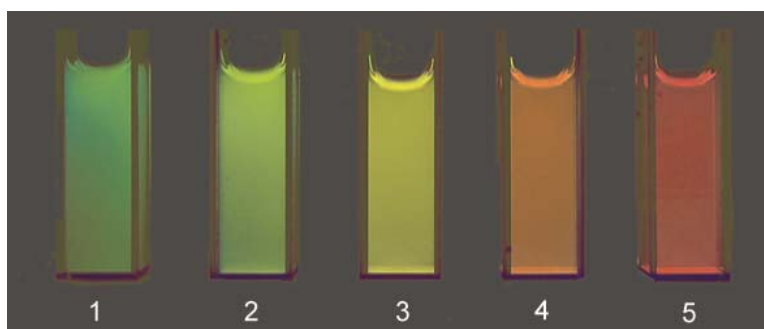


Figure 2. Photographic picture of the fluorescence of suspensions **1-5** after specific excitation of the pyronine illustrating the increasing pyronine to oxonine energy transfer rate from left to right. The dye concentration inside the nanocrystals increases from left to right.

The main processes responsible for the observation in Figure 2 are explained in Figure 3. Energy migration between the donor molecules and between the acceptor molecules, which are of similar probability as the energy transfer, and also radiationless relaxation processes are not indicated.

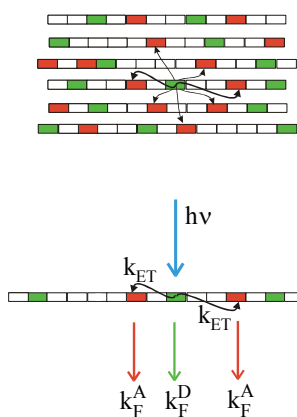


Figure 3. Main processes taking place in a zeolite L nanocrystal containing a mixture of donor (pyronine) and acceptor (oxonine) molecules, after excitation of a donor. k_{ET} is the rate constant for energy transfer, while k_F^A and k_F^D are the rate constants for fluorescence of the acceptor and the donor, respectively. The donor molecules are marked as green rectangles and the acceptors as red rectangles.

Taking into account radiationless processes, namely internal conversion k_{IC} , intersystem crossing k_{ISC} , and bimolecular quenching $k_Q[Q]$ with a quencher Q, the time dependent concentrations of the donor D and the acceptor A in the excited singlet state S_1 , $[D_{S_1}]$ and $[A_{S_1}]$, can be expressed as follows, where j_{abs} is the number of photons absorbed per unit time:

$$\frac{d[D_{S_1}]}{dt} = j_{abs} - (k_{Et} + k_F^D + k_{IC}^D + k_{ISC}^D + k_Q^D[Q])[D_{S_1}] = j_{abs} - [D_{S_1}] \sum k_d^D \quad (2)$$

$$\frac{d[A_{S_1}]}{dt} = k_{Et}[D_{S_1}] - (k_F^A + k_{IC}^A + k_{ISC}^A + k_Q^A[Q])[A_{S_1}] = k_{Et}[D_{S_1}] - [A_{S_1}] \sum k_a^A \quad (3)$$

From this follows the fluorescence quantum yield of the donor Φ_F^D and of the acceptor Φ_F^A , under stationary conditions:

$$\Phi_F^D = \frac{k_F^D}{\sum k_d^D} \quad (4)$$

$$\Phi_F^A = \frac{k_{Et}}{\sum k_d^D} \frac{k_F^A}{\sum k_a^A} \quad (5)$$

A quantity which in many cases can easily be measured, even in a heterogeneous system, is the ratio between these two fluorescence quantum yields. We therefore write:

$$\frac{\Phi_F^A}{\Phi_F^D} = k_{Et} \frac{k_F^A}{k_F^D \sum k_a^A} \quad (6)$$

This equation shows that the ratio between the acceptor and donor fluorescence quantum yields is directly proportional to the energy transfer rate constant k_{Et} . Applying Försters equation²⁴, the rate constant k_{Et}^{ij} for energy transfer from an excited dye molecule on site i to an unexcited one on site j depends on the fluorescence quantum yield Φ_i of the donor in absence of acceptors, on its natural lifetime τ_i , on the refractive index n of the medium, on the geometrical factor G_{ij} , on the spectral overlap J_{ij} of the donor emission and the acceptor absorption spectra, and on the occupation probabilities p_i and p_j of the respective sites. N_A is the Avogadro number.¹²

$$k_{Et}^{ij} = \frac{9(\ln 10)}{128\pi^5 N_A n^4} \frac{\Phi_i}{\tau_i} G_{ij} J_{ij} p_i p_j \quad (7)$$

The spectral overlap J_{ij} is equal to the integral of the corrected and normalized fluorescence intensity $f_i(\bar{\lambda})$ of the donor multiplied by the extinction coefficient $\varepsilon_j(\bar{\lambda})$ of the acceptor as a function of the wavenumber $\bar{\lambda}$:

$$J_{ij} = \int_0^\infty \varepsilon_j(\bar{\lambda}) f_i(\bar{\lambda}) \frac{d\bar{\lambda}}{\bar{\lambda}^4} \quad (8)$$

The absorption and fluorescence spectra of pyronine and oxonine in Figure 4 illustrate the large pyronine/pyronine, pyronine/oxonine and oxonine/oxonine spectral overlap which

is one of the reasons why these dyes are well suited for the experiments discussed in this article.

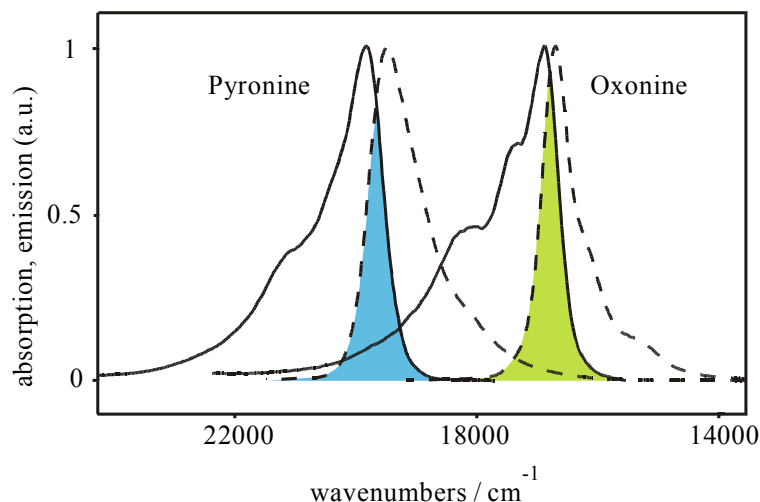


Figure 4. Absorption (solid) and corrected emission (dotted) spectra of Py—L and Ox—L suspended in water. The maxima of all spectra were adjusted to equal height. The spectral overlap of the two dyes are shaded; the pyronine/oxonine spectral overlap is not marked.

The geometrical factor G_{ij} takes into account the influence of the geometrical arrangement of a donor i and an acceptor j . It depends on the distance R_{ij} and on κ_{ij} . The latter describes the relative orientation in space of the transition dipole moments $(\mu_{S_1 \leftarrow S_0})_i$ and $(\mu_{S_1 \leftarrow S_0})_j$ of the donor i and of the acceptor j , respectively:

$$G_{ij} = \frac{\kappa_{ij}^2}{R_{ij}^6} \quad (9)$$

The rate constant k_{Et}^d can be expressed as follows, for an energy transfer from an excited donor \mathbf{d} to acceptors \mathbf{a} as illustrated in Figure 3:

$$k_{Et}^d = \sum_a k_{Et}^{da} = \frac{9(\ln 10)}{128\pi^5 N_A n^4} \frac{\Phi_d}{\tau_d} \sum_a G_{da} J_{da} p_a \quad (10)$$

In this equation p_a is equal to one and does therefore not appear, because we describe energy transfer from a donor which is excited with a probability equal to one. In addition, we average over many such events taking place in many different nano crystals with similar geometrical environment $\langle \sum_a G_{da} \rangle$. Since J_{da} also appears as an average quantity, eq (10) can be simplified as follows:

$$k_{Et}^d = \frac{9(\ln 10)}{128\pi^5 N_A n^4} \frac{\Phi_d}{\tau_d} \langle J_{da} \rangle \langle \sum_a G_{da} \rangle p_a \quad (11)$$

Inserting this expression into (6), we obtain:

$$\frac{\Phi_F^A}{\Phi_F^D} = \left\{ \frac{k_F^A}{k_F^D \sum k_d^A} \frac{9(\ln 10)}{128\pi^5 N_A n^4} \frac{\Phi_d}{\tau_d} \langle J_{da} \rangle \langle \sum_a G_{da} \rangle \right\} p_a \quad (12)$$

This equation tells us that the ratio of the acceptor to donor luminescence quantum yield is proportional to the donor occupation probability. Provided that all values in the curved brackets are kept constant we can write:

$$\frac{\Phi_F^A}{\Phi_F^D} = C p_a \quad (13)$$

where C is equal to:

$$C = \frac{k_F^A}{k_F^D \sum k_d^A} \frac{9(\ln 10)}{128\pi^5 N_A n^4} \frac{\Phi_d}{\tau_d} \langle J_{da} \rangle \langle \sum_a G_{da} \rangle \quad (14)$$

Equation (13) can best be tested by carrying out the second type of experiments mentioned at the beginning of this chapter, namely by working with a constant amount of zeolite L but by varying the amount of oxonine and pyronine. Under these conditions light scattering is constant. The results of such an experiment are illustrated in Figure 5 for occupations $p_a \approx 2^a \times 0.0015$, $a = 0, 1, 2, 3$, and 4, which correspond to dye concentrations inside of each nanocrystal of $2^a \times 0.0006$ M. The experiment was carried out with zeolite L of 700 nm average length. The fluorescence spectra on the left side of Figure 5, measured after specific excitation of the pyronine, show that at the lowest loading the green emission of the pyronine with maximum at about 520 nm dominates. However, an increase of the loading causes this emission to decrease and the oxonine emission with a maximum at about 605 nm to increase. At highest loading $p = 0.0288$, which is still low, the oxonine emission clearly dominates. The ratio of the acceptor to donor fluorescence intensity illustrated on the right side of Figure 5 shows that the linear relation, eq 13, holds with a constant $C = 120$. The bathochromic shift of the maximum of the pyronine emission band is due to self-absorption and reemission.^{10,25-27} Data reported in ref 9 for experiments carried out in a slightly different way show the same behavior.

Energy transfer in the channels of zeolite L as illustrated in Figures 2 and 5 can also be used for measuring the insertion kinetics. For this a situation as illustrated in Figure 6 is prepared at the beginning of the experiment. Immediately after all dye molecules have entered the zeolite channels maximum energy transfer is observed because the donor to acceptor distance is short. When the molecules diffuse into the zeolite the donor to acceptor distance increases and hence the energy transfer rate decreases. From this the insertion kinetics can be derived. We have carried out such experiments successfully which will be reported elsewhere.²⁹ A different approach was used for measuring the exit kinetics of an anionic dye.³⁰

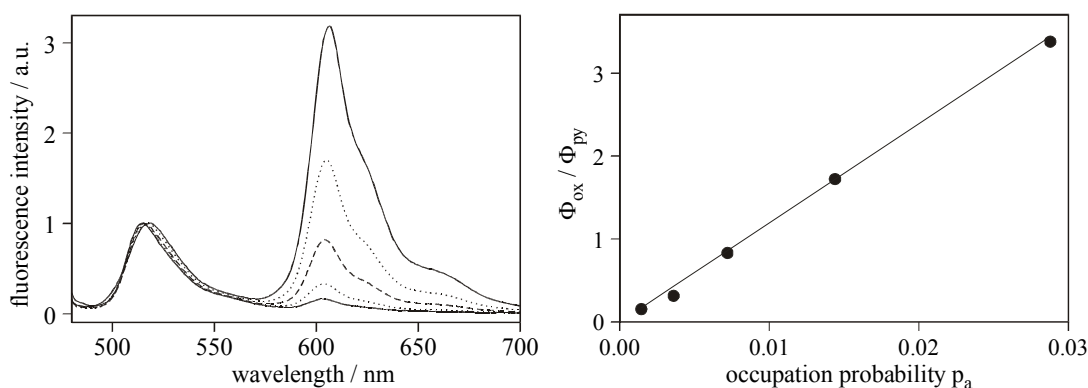


Figure 5. Fluorescence spectroscopic examinations of 5 suspensions with $p_a = 0.0014$, 0.0036, 0.0072, 0.0144 and 0.0288 after specific excitation of the pyronine at 465 nm. Left: Fluorescence spectra normalized to the same peak height for the pyronine emission (band on the left at about 520 nm). The intensity of the oxonine emission (peak on the right) increases with increasing p_a . Right: Ratio of the fluorescence intensity Φ_{ox} of the acceptor (oxonine) and the donor (pyronine) Φ_{py} as a function of the loading p_a of the zeolite L.²⁸

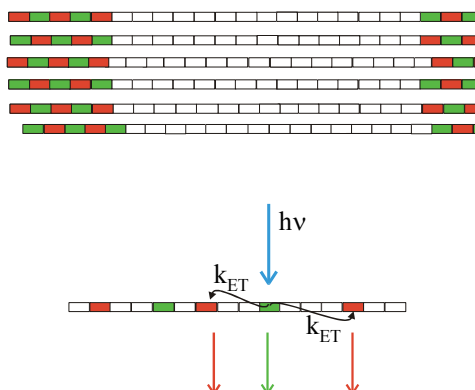


Figure 6. Zeolite L microcrystal for measuring the intrazeolite diffusion of dye molecules by means of Förster energy transfer. Above: the situation at the beginning of the experiment. Below: compare with Figure 3. The donor molecules are marked as green rectangles and the acceptors as red rectangles.

4. EXCHANGE EQUILIBRIUM

In the experiments described here insertion of the cationic dyes into the zeolite L channels was realized by means of ion exchange. For monovalent cations the exchange equilibrium is described by:



where X_S^+ and M_S^+ denote the dye cation and the metal cation in solution. Z stands for zeolite and Y describes the cation concentration inside of the zeolite. For monovalent cations and dyes which occupy two unit cells in zeolite L we must use $Y_{n_{box}-r} = \left[(M_{18}^+)_{n_{box}-r} (M_{17}^+)_r \right]$. The parameter n_{box} is equal to the number of sites in one channel and r counts the number of sites occupied by a dye. For e.g. a 300 nm long zeolite n_{box} is equal to 200 because the length of a site is 1.5 nm for oxonine and pyronine. Equilibrium (15) corresponds to the situation expressed in the eqs (26) to (29) of our study on particle distribution in microporous materials.³¹ This means that the equilibrium constant K_r can be expressed as:

$$K_r = \frac{[ZY_{n_{box}-r}X_r][M_S^+]}{[ZY_{n_{box}-(r-1)}X_{r-1}][X_S^+]} \quad (16)$$

We have shown that K_r depends as follows on r because the entropy of the system decreases with increasing loading (see Table 1 of ref 31):

$$K_{r+1} = K_r \left[\frac{r+1}{r} \frac{n_{box}-r+1}{n_{box}-r} \right]^{-1} \quad (17)$$

Table 1: Equilibrium constants K_r and entropy change in J/(Kmol)

r	1	2	3	4	5	6	7	8	9	10	11	12
K_r	1.	.458	.278	.178	.133	.097	.071	.052	.037	.025	.015	6.94×10^{-3}
ΔS_r	0.	-6.49	-10.6	-13.9	-16.8	-19.4	-21.9	-24.6	-27.4	-30.7	-34.8	-41.3

The dependence of the equilibrium constant K_r as a function of the occupation probability for $K_1 = 3500$ shown in Figure 7 illustrates that ion exchange is complete for low loading, but that the situation changes for higher loading. This fact must be taken into account when doing experiments of the type described in this article.

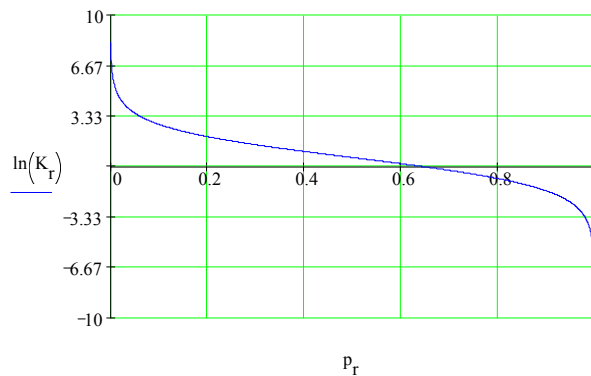


Figure 7. Equilibrium constant for ion exchange of a monovalent cation in zeolite L with a cationic dye molecule with charge +1, as a function of the occupation probability p_r , calculated for $K_1 = 3500$.

5. VERY FAST ENERGY MIGRATION

We have recently reported extremely fast electronic excitation energy migration along the axis of cylindrical crystals of pyronine loaded zeolite L nano crystals modified on both ends with oxonine as luminescent traps. We have good evidence that the antenna property of this system is governed by Förster-type energy migration. It is supported by an increase of the effective excitation lifetime because of donor-donor self-absorption and reemission.^{10,28}

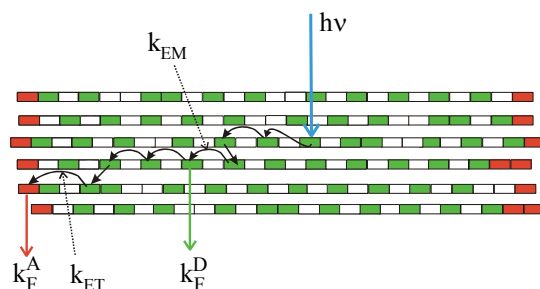


Figure 8. Main processes occurring in the energy migration from an excited donor (pyronine) taking place mainly along the cylinder axis because of geometrical constraints. The excitation energy is finally trapped by an acceptor (oxonine) located at the end of the zeolite L nanocrystal which emits red light. k_{ET} is the rate constant for energy transfer, while k_F^A and k_F^D are the rate constants for fluorescence of the acceptor and the donor, respectively. The donor molecules are marked as green rectangles and the acceptors as red rectangles.

Two kinds of stationary experiments give useful information: one is to measure the trapping efficiency as a function of the loading and the other is to measure it as a function of the length of the nano crystals. Both have been carried out by us.¹⁰ The trapping efficiency T_∞ is equal to the sum of the excitation probabilities of all trapping sites at infinite time after irradiation. In a system where donors and traps have a luminescence quantum yield of one and where the traps are excited exclusively by receiving energy from the donors, the trapping efficiency corresponds to the ratio of the luminescence intensity of the traps divided by the total luminescence. In the experiments described here, the donors which absorb light are pyronine while the traps are oxonine molecules. Their luminescence intensity is given by I_{py} and I_{ox} , respectively. We have shown that for this system the following simple relation holds.^{10,12}

$$T_\infty = \frac{I_{ox}}{I_{py} + I_{ox}} \quad (1)$$

An experiment which demonstrates the extremely fast energy migration is illustrated in Figure 9. In this experiment effective energy migration lengths of up to 166 nm were observed; see Table 1 of ref 10. Note that only the emission maximum of the donor (pyronine) shifts to longer wavelength with increasing loading. The emission maximum of the acceptor which is oxonine, placed at both ends of the cylindrical crystals, does not shift. The reason for this is that its concentration is always low and the same in each experiment. We have recently improved the material and the experimental techniques and we have observed migration lengths of up to about 200 nm on thin dye-zeolite layers coated on glass.⁸

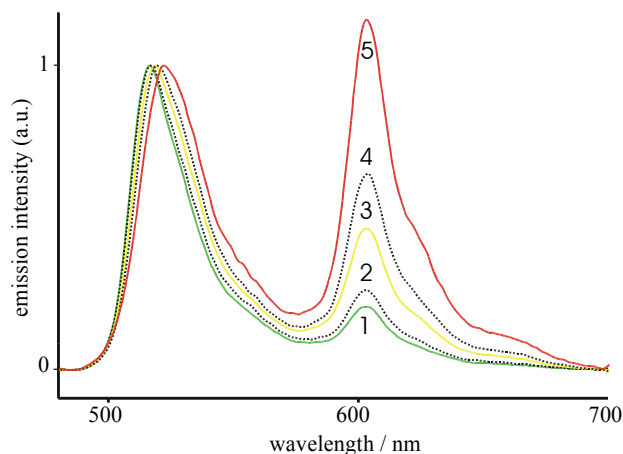


Figure 9. Energy migration in pyronine-loaded nano crystals as observed by the oxonine fluorescence at different pyronine loading p_{py} , increasing from **1** to **2**, **3**, **4**, **5** by a factor of about 2 each time; $p_{py}(\mathbf{1}) \approx 0.03$. We show the relative intensity of fluorescence spectra recorded after specific excitation of only pyronine molecules at 470 nm scaled to the same height at the maximum of the pyronine emission. The amount of front-back located oxonine traps corresponds on average to one molecule at the front and one at the back of each channel in all samples.

6. EXTERNAL TRAPPING

So far experiments on energy transfer, energy migration and trapping taking place inside of the dye loaded zeolite nano crystals have been discussed. In order to realize devices of the type illustrated in Figure 1 radiationless energy transfer to an external acceptor is needed. The principle of an experiment to probe for energy transfer to a trap located at the outside of a nanocrystal is illustrated in Figure 10. Energy is absorbed by a donor located somewhere inside of the crystal, it then migrates very fast to one of the ends of the cylinder where it is trapped by an acceptor which itself is able to transfer the energy to an external acceptor. The internal acceptor is not necessary but it is convenient in many cases.

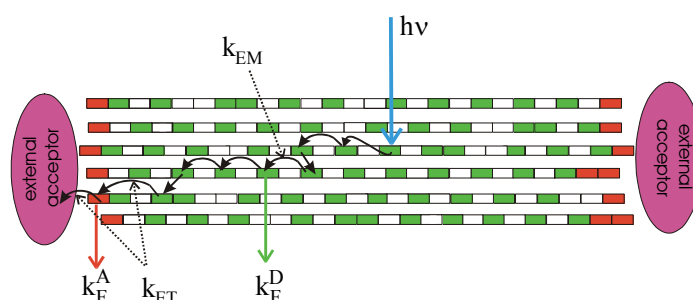
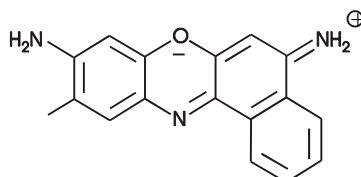


Figure 10. External trapping of energy absorbed somewhere by a donor inside of a dye loaded zeolite nanocrystal. Energy migration takes place mainly along the cylinder axis because of geometrical constraints. The excitation is trapped by an acceptor located at the end of the zeolite L nanocrystal. The excited acceptor either transfers its energy to an external acceptor or relaxes by emitting a photon, depending on the conditions.

We have carried out a number of such experiments from which I report two relatively simple ones, both realized without an internal acceptor. The first consists of placing a molecule which is too large to enter the channels of zeolite L at the surface. This molecule should have a large spectral overlap with the donor molecules located inside of the nano crystals. We know that cationic dyes such as methyleneblue, ethyleneblue, cresylviolet and others readily adsorb at the zeolite L nano crystal surface and that they do not enter the channels.³² Here we show an experiment in an aqueous dispersion carried out with cresylechtviolet, the formula of which is given in Scheme 3. The results illustrated in Figure 11 show that external trapping works well. Experiments with methyleneblue as an external trap lead to similar results.²¹



Scheme 3: Cresylechtviolet used as an external quencher molecule.

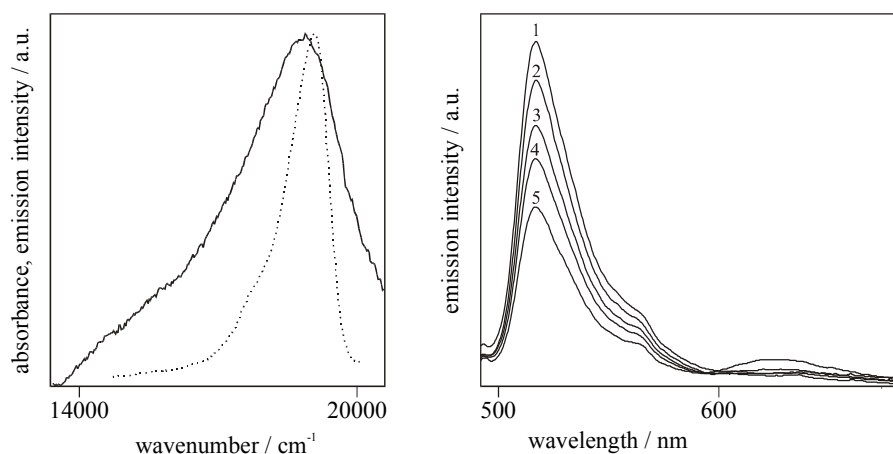


Figure 11. Left: Spectral overlap between the absorption spectrum of the external quencher (cresylechtviolet, solid) and the fluorescence spectrum of internal donor (pyronine, dotted). Right: Fluorescence of the pyronine as a function of the cresylechtviolet adsorbed on the outside of the nano crystals. The pyronine loading was about 0.006. The amount of cresylechtviolet on the outside increases from 1 to 2,3,4,5. Its concentration was so low, that absorption of the pyronine luminescence by the quencher remained unimportant.^{21,33}

The second experiment I would like to report was carried out on a thin oxonine loaded zeolite L layer on glass onto which in one case different amounts of gold and in the other case different amounts of silicon were evaporated. In both cases quenching of the oxonine luminescence was observed, which was however, more pronounced in the case of gold. Results on the quenching of the oxonine fluorescence as a function of the amount of gold deposited onto the zeolite nano crystals are reported in Figure 12 for two different oxonine loading. Care was taken that light absorption by the gold deposited on the nanocrystal did not disturb the experiment. I would like to draw attention in this context to the optical pumping of dye-complexed and -sensitized porous silicon increasing photoemission rates.³⁵

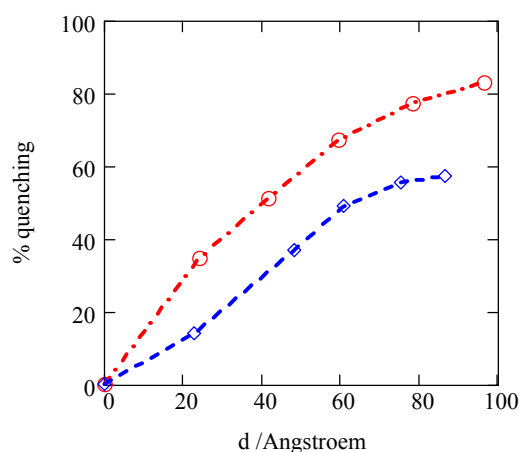


Figure 12. Quenching of the oxonine luminescence of an oxonine loaded zeolite L nano crystals coated as a thin layer on glass by vapor deposited gold. The oxonine loading was about 0.065 (circles) and 0.025 (diamonds). The absolute thickness d of the gold layer given in Å could not be measured precisely in these experiments but the estimated values are sufficiently precise.³⁴

We conclude that the fascinating properties of the systems discussed in this article give rise to many speculations on applications. The antenna properties can perhaps be used in realizing a new type of photovoltaic devices in which the absorption of light and the creation of an electron-hole pair are spatially separated, as illustrated in Figure 1. Contributions to new imaging techniques, data storage, specific biological and medical applications can be imagined. The antenna nano crystals can also be regarded as candidates for realizing a new type of electronic screen with high spatial resolution. The extremely fast energy migration, the pronounced anisotropy, the geometrical constraints, and the high concentration of monomers which can be realized bear much potential in leading to new photo physical phenomena.

ACKNOWLEDGMENT

This work was supported by the Swiss National Science Foundation Project NFP 36(4036-043853), project NF 2000-053414/98/1 and by the Bundesamt für Energiewirtschaft, Projekt 10441. I would like to thank David Schürch and Michel Pfenniger for reading this manuscript carefully.

REFERENCES AND NOTES

- [1] Meier, W.M.; Olson, D.H.; Baerlocher, Ch. *Atlas of Zeolite Structure Types*; Elsevier; London 1996.
- [2] Breck, D.W. *Zeolite Molecular Sieves*; John Wiley & Sons: New York, 1974.
- [3] Ohsuna, T.; Horikawa, Y.; Hiraga, K. *Chem. Mater.* **1998**, 10, 688.
- [4] Kühlbrandt, W.; Wang, D.N. *Nature* **1991**, 350, 130.
- [5] Fetisova, Z.G.; Freiberg, A.M.; Timpmann, K.E. *Nature* **1988**, 334, 633.
- [6] Sundström, V.; Pullerits, T.; van Grondelle, R. *J. Phys. Chem B* **1999**, 103, 2346.
Arnette, D.C.; Moser, C.C.; Dutton, P.L.; Scherer, N.F. *ibid* 2014. Vulto, S.I.E.; Kennis, J.T.M.; Streltsov, A.M.; Amesz, J.; Aartsma, T.J. *ibid* 878.
- [7] Calzaferri, G. *Chimia* **1998**, 52, 525.
- [8] Megelski, S.; PhD Thesis 2000, University of Berne **2000**.
- [9] Gfeller, N.; Megelski, S.; Calzaferri, G. *J. Phys. Chem B* **1998**, 102, 2433.
- [10] Gfeller, N.; Megelski, S.; Calzaferri, G. *J. Phys. Chem B* **1999**, 103, 1250.
- [11] Hennessy, B.; Megelski, S.; Marcolli, C; Shklover, V.; Bäerlocher, Ch.; Calzaferri, G. *J. Phys. Chem. B* **1999**, 103, 3340.
- [12] Gfeller, N.; Calzaferri, G. *J. Phys. Chem. B* **1997**, 101, 1396.
- [13] Vietze, U.; Krauss, O.; Laeri, F.; Ihlein, G.; Schüth, F.; Limburg, B.; Abraham, M. *Phys. Rev. Letters* **1998**, 81, 4628.
- [14] Balzani, V.; Campagna, S.; Denti, G.; Juris, A.; Seroni, S.; Venturi, M. *Acc. Chem. Res.* 1998, 31, 26.
- [15] Yamazaki, I.; Tamai, N; Yamazaki, T. *J. Phys. Chem* **1990**, 94, 516.
Bücher, H.; Drexhage, K.H.; Fleck, M.; Kuhn, H.; Möbius, D.; Schäfer, F.P.; Sondermann, J.; Sperling, W.; Tillmann, P.; Wiegand, J. *Mol. Cryst.* **1967**, 2, 199.
- [16] Lainé, P.; Lanz, M.; Calzaferri, G. *Inorg. Chem.* **1996**, 35, 3514.
- [17] Bockstette, M.; Wöhrle, D.; Braun, I.; Schulz-Ekloff, G. *Microp. Mesop. Mater.* **1998**, 23, 83.
- [18] Schüth, F. *Chemie i.u. Zeit* **1995**, 29, 42.
- [19] Ramamurthy, V., Photochemistry in Organized & Constrained Media, VCH Inc. 220 East 23rd Street, Suite 909, New York 1991. Ramamurthy, V. *Chimia* **1992**, 46, 359.
- [20] Ehrl, M.; Deeg, F. W.; Bräuchle, C.; Franke, O.; Sobbi, A.; Schulz-Ekloff, G.; Wöhrle, D. *J. Phys. Chem.* **1994**, 98, 47. Caro, J.; Marlow, F.; Wübbenhorst, M. *Adv.Mater.* **1994**, 6, 413. Wöhrle, D.; Schulz-Ekloff, G. *Adv.Mater.* **1994**, 6, 875. Hoffmann, K.; Marlow, F.; Caro, J. *Zeolites* **1996**, 16, 281.
- [21] Binder, F.; Calzaferri, G.; Gfeller, N. *Sol. Ener. Mat. Sol. Cells* **1995**, 38, 175.
Binder, F.; Calzaferri, G.; Gfeller, N. *Proc. Ind. Acad. Sci (Chem.Sci)* **1995**, 107, 753.
- [22] Kuhn, H. *J. Chem. Phys.* **1970**, 53, 101.
- [23] Lainé, P.; Seifert, R.; Giovanoli, R.; Calzaferri, G. *New. J. Chem.* **1997**, 21, 453.
- [24] Förster, Th. *Ann. Phys (Leipzig)* **1948**, 2, 55. Förster, Th. *Fluoreszenz organischer Verbindungen*; Vandenhoeck & Ruprecht; Göttingen 1951.
- [25] Baumann, J.; Calzaferri, G.; Hugentober, T. *Chem. Phys. Letters* **1985**, 116, 66.
- [26] Hammond, P.R. *J. Chem. Phys.* **1979**, 70, 3884.
- [27] Batchelder, J.S.; Zewail, A.H.; Cole, T. *Applied Optics* **1979**, 18, 3090.

- [28] Calzaferri, G.; Brühwiler, D.; Megelski, S.; Pfenniger, M.; Pauchard, M.; Hennessy, B.; Maas, H.; Devaux, A.; Graf, U. *Solid State Sciences*, 2, **2000**, 421.
- [29] Pfenniger, M.; Calzaferri, G. *ChemPhysChem* **2000**, 1, 211
- [30] Brühwiler, D.; Gfeller, N.; Calzaferri, G.; *J. Phys. Chem B* **1998**, 102, 2923.
- [31] Kunzmann, A.; Seifert, R.; Calzaferri, G. *J. Phys. Chem. B* **1999**, 103, 18.
- [32] Calzaferri, G.; Gfeller, N. *J. Phys. Chem.* **1992**, 96, 3428.
- [33] Binder, F. PhD Thesis, University of Berne **1996**.
- [34] van der Wielen, M. part of Diploma Thesis, University of Berne **1995**.
- [35] Gole, J.L. DeVincentis, J.A.; Seals, L. *J. Phys. Chem. B* **1999**, 103, 979.